processes

MDPI

Article

Geochemical Characteristics and Hydrocarbon Generation Potential of Coal-Measure Source Rocks in Julu Sag

Yang Wang [1,2,*], Hanyu Zhang [1,2], Liu Yang [3], Yanming Zhu [1,2] and Zhixiang Chang [1,2]

[1] Key Laboratory of Coalbed Methane Resources and Reservoir Formation Process, Ministry of Education, China University of Mining and Technology, Xuzhou 221008, China; h9798@cumt.edu.cn (H.Z.); h2001r0112@cumt.edu.cn (Y.Z.); ts23010041a31@cumt.edu.cn (Z.C.)
[2] School of Resources and Geoscience, China University of Mining and Technology, Xuzhou 221116, China
[3] School of Construction Management, Jiangsu Vocational Institute of Architectural Technology, Xuzhou 221116, China; l0043y@cumt.edu.cn
* Correspondence: wangy89@cumt.edu.cn; Tel.: +86-15896422124

Abstract: To uncover the reservoir characteristics and enrichment law of coal-measure gas in Julu sag, Hebei Province, and achieve co-exploration and co-mining, it is necessary to conduct a comprehensive analysis. In this study, we investigated the characteristics of coal-measure gas accumulation in the Taiyuan Formation and Shanxi Formation in the Julu area. This was achieved by collecting data on coal-measure source rocks and organic geochemistry, which were then combined with regional geological conditions. This study indicates that the coal seams and shales of Shanxi Formation and Taiyuan Formation in the study area serve as the primary source rocks. The predominant macerals found in coal rock are vitrinite. Furthermore, the organic matter type present in shale is primarily categorized as type II_2, with the organic matter maturity falling within the immature–mature stage. Based on the simulation results of tectonic-burial history, thermal evolution history, and hydrocarbon generation history in the study area, it is evident that the coal-measure source rocks experienced their first peak of hydrocarbon generation during the Mesozoic era as a result of deep metamorphism. Subsequently, the area experienced uplift and erosion, leading to the release of coal-bearing natural gas. Since the Paleogene period, the coal-bearing source rocks have undergone sedimentary burial and entered the secondary hydrocarbon generation stage, resulting in significant production of oil and gas. Based on the analysis of gas content, buried depth, source rock thickness, and sealing conditions in the study area, it is evident that the potential of coal-measure gas resources in the study area is primarily comprised of shale gas with supplementary coalbed methane. It can be inferred that the deeper areas within the study area hold greater exploration prospects.

Keywords: Julu sag; coal-measure gas; source rock; tectonic evolution; hydrocarbon generation evolution

Citation: Wang, Y.; Zhang, H.; Yang, L.; Zhu, Y.; Chang, Z. Geochemical Characteristics and Hydrocarbon Generation Potential of Coal-Measure Source Rocks in Julu Sag. *Processes* **2024**, *12*, 1399. https://doi.org/10.3390/pr12071399

Academic Editor: Carlos Sierra Fernández

Received: 11 June 2024
Revised: 28 June 2024
Accepted: 3 July 2024
Published: 4 July 2024

1. Introduction

Coal-measure gas refers to natural gas that is produced through the biochemical and physical chemistry processes of source rocks in coal-measure strata during the formation of coal. This includes coalbed methane, shale gas, tight sandstone gas, and other unconventional natural gas resources that exist within coal-measure strata [1,2]. Coal and dark carbonaceous mud shale, as source rocks in coal-measure formations, exhibit characteristics of 'homogenous symbiosis and interbedded cycles', which contribute to the coupled accumulation of coal-measure gas [3]. In recent years, China has intensified its efforts in the exploration and development of unconventional natural gas, resulting in significant achievements and advancements in coalbed methane, shale gas, and tight-sandstone gas. Currently, research on the hydrocarbon generation and expulsion laws, accumulation mechanisms, accumulation and dispersion laws, reservoir characteristics, and comprehensive exploration and production methods of coal-measure gas source rocks is still ongoing [4–11]. However, the research on coal-measure gas symbiosis and superposition as

well as coal-measure gas co-exploration and co-production is still in its early stages. Based on previous studies, coal-measure gas symbiotic assemblages can be broadly categorized into three groups: self-generation and co-storage, self-generation and self-storage, and symbiotic assemblages. The symbiotic assemblage is intricately regulated by variations in regional distribution, depositional environment, diagenesis, tectonism, and assemblage conditions [12–16].

The burial history and thermal evolution process of hydrocarbon source rocks has emerged as a focal point of research in the field of earth science. This topic has garnered significant attention due to its implications for understanding the formation and maturation of hydrocarbon reservoirs [17–20]. Basin modeling analysis can provide insight into the hydrocarbon generation potential of a specific basin, offering valuable guidance for the exploration and development of oil and gas resources. This information is crucial for making informed decisions in the energy industry. This method integrates geological and geochemical parameters (Including formation thickness, deposition rate, paleo heat flow, abundance of organic matter, vitrinite reflectance, and so on) to assess the efficiency of hydrocarbon generation in source rocks and determine the evolution process of organic matter during hydrocarbon generation [19,20]. The purpose of basin modeling analysis is to reconstruct the structural burial history of the basin by simulating its evolution, estimating the timing and extent of hydrocarbon generation from source rocks, identifying oil and gas migration pathways, and analyzing the process of oil and gas accumulation. This has significant implications for assessing the generation and expulsion of hydrocarbons in sedimentary basins [17–20]. Therefore, in order to elucidate the process of gas generation and the resource potential of coal-bearing strata, it is essential to reconstruct the tectono–thermal evolution history of the Julu sag since the late Paleozoic, taking into account geochemical parameters.

The coal-measure strata in the Julu-Guangzong area of Hebei Province consist mainly of sea–land alternating facies within the Carboniferous–Permian Taiyuan Formation–Shanxi Formation. The lithology of the coal-measure strata is highly variable, consisting primarily of coal, carbonaceous mudstone, mud shale, and interbedded sandstone. This lithology is widely distributed, with significant thickness and stable vertical changes. Due to the diverse lithology of coal-measure strata and their various combinations, as well as the presence of rich coal-measure gas symbiotic combination models and complex gas-bearing systems, this area exhibits significant potential for coal-measure gas resources [21–23]. The study area is situated in the western part of the Linqing depression. The predecessors have conducted extensive research on the structural evolution characteristics and laws of oil and gas accumulation in the Linqing depression. They have investigated the stratigraphic distribution, analyzed the structural characteristics of the Linqing depression, defined a multi-stage structural evolution process, and discussed the development characteristics of upper Paleozoic source rocks [24–27]. However, the level of exploration in the Julu Sag is generally low, with weak research on accumulation conditions and an unclear tectonic evolution history. These factors have hindered the exploration and development of coal-measure gas in this area.

The primary purpose of this study is threefold: (1) to reveal and compare the hydrocarbon generation capacity and hydrocarbon generation intensity of source rocks in the Taiyuan Formation and Shanxi Formation based on organic geochemistry analysis; (2) the burial history, thermal evolution history, and hydrocarbon generation model of the coal-measure strata in Julu sag were established by combining geochemical data with structural stratigraphic information collected from drilling data. This was achieved using PetroMod 1D (2012.2) software; and (3) to establish the co-generation reservoir model of coal-measure gas in Julu sag and to determine the optimal conditions for the enrichment and accumulation of coal-measure gas. Our study holds significant importance in evaluating the hydrocarbon generation potential of coal-bearing gas in Julu sag, and it provides a theoretical basis for the exploration of coal-bearing gas reservoirs in Julu sag.

2. Geological Settings

The Linqing Depression is situated in the southwest of the Bohai Bay Basin, which is a secondary structural unit within the basin. The overall trend of the Linqing depression's distribution is oriented between NNE and NE. It has undergone a Mesozoic–Cenozoic rifted basin and has been affected by multiple stages of tectonic movements, resulting in superposition [28]. The western side of the Linqing depression is characterized by the uplift area of the Taihang Mountains, while the eastern side features the Luxi uplift. To the north, it is adjacent to the Xingheng uplift as well as the Jizhong, Jiyang, and Huanghua depressions. Meanwhile, to the south lies the Neihuang uplift. Within the depression, there are two fault zones: the Huilongzhen–Maling fault and the Yaozhan fault. There are 11 depressions, including Dongpu depression, Xinxian depression, and Julu depression, as well as 7 bulges such as Guantao uplift, Tangyi uplift, and Guangzong uplift. In total, there are 18 secondary structural units. There are a total of 7 uplifts, which include 18 secondary tectonic units. The overall characteristics exhibit an east–west zoning and north–south block pattern [29,30] (Figure 1a).

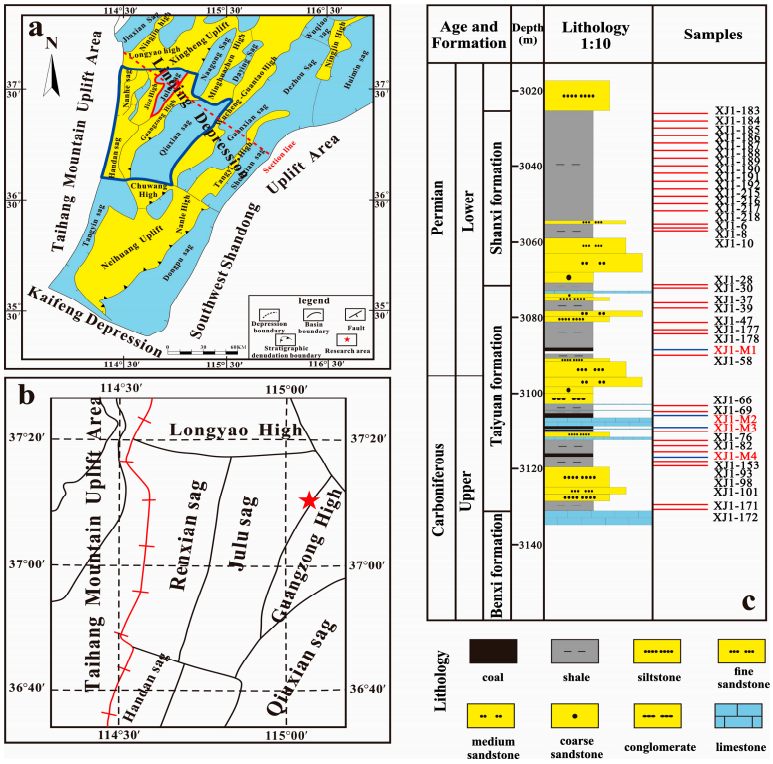

Figure 1. Geological structure sketch of the Linqing Depression and borehole lithology histograms. (**a**) structural unit division map of Linqing depression; (**b**) the tectonic unit division map of the study area; (**c**) the stratigraphic column and sample point map of Well XJ1.

The study area consists of two secondary structural units, namely the Julu Sag and the Guangzong Bulge. These units make up the main body of the study area. The Julu Sag, situated in the northwest of the Linqing Depression, is a secondary structural unit of the Linqing Depression. It is bordered by the Longyao uplift to the north, with the Longyao fault serving as the boundary; by the Guangzong uplift to the east, with a fault zone as its boundary; by the Renxian sag to the west, with the Xingjiawan fault zone as its boundary; and by the Handan sag to the south, with the Linzhang Weixian fault as its boundary (Figure 1b). The stratigraphic development characteristics of this area are relatively consistent with those in the region. The strata developed from old to new, including the Middle Ordovician Fengfeng Formation, Carboniferous–Permian Benxi Formation, Taiyuan Formation, Shanxi Formation, Lower Shihezi Formation, Upper Shihezi

Formation, Shiqianfeng Formation, Triassic Liujiagou Formation, Heshanggou Formation, Ermaying Formation, and Cenozoic Neogene and Quaternary (Figure 2). In general, the Late Paleozoic strata are relatively well preserved, while the Early Paleozoic and Mesozoic strata are notably absent [30–33]. The focus of this study is the Upper Paleozoic source rock, which consists of coal-rock lacustrine mudstone and carbonaceous mudstone from the Taiyuan-Shanxi Formation.

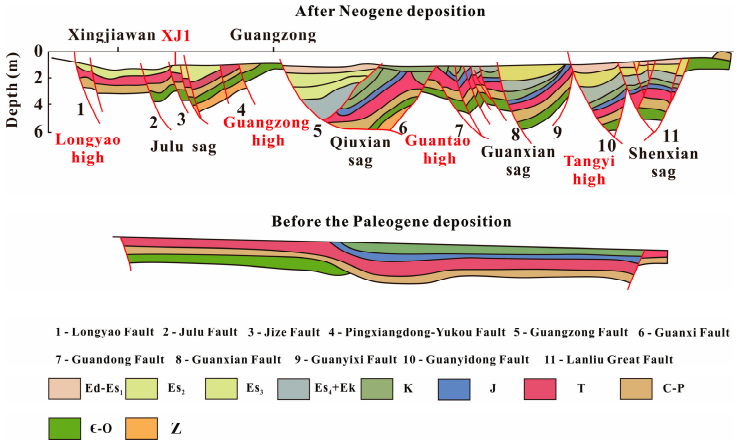

Figure 2. Structural evolution profile of Linqing depression (Longyao—Shenxian section).

3. Organic Geochemical Characteristics of Source Rocks

Organic geochemical parameters are effective in evaluating the intensity and capacity of hydrocarbon generation in source rocks. This is particularly important for assessing the potential for hydrocarbon production. To assess the hydrocarbon generation potential and intensity of the source rocks in the study area, organic geochemical analysis was conducted on coal and shale samples collected from the Shanxi and Taiyuan formations. This analysis determined the coal quality, coal type, organic matter type, organic matter abundance, and organic matter maturity of the source rock.

3.1. Samples and Experimental Method

A total of 39 representative samples were collected and analyzed in this study: 17 samples from the Shanxi Formation and 22 samples from the Taiyuan Formation. The samples were obtained from the shale core of Well XJ1, with sampling depths ranging between 3026 and 3140 m. The specific burial depths of the samples are outlined in Table 1, and the primary lithology of the samples consists of coal, shale, and carbonaceous shale (Figure 1c).

Table 1. The organic matter content (TOC), vitrinite reflectance (R_O), and maceral data of coal and shale samples.

Stratum	Sample No.	Depth (m)	TOC (%)	R_O (%)	Vitrinite (%)	Inertinite (%)	Exinite (%)
Shanxi Formation	XJ1-183	3026.31	6.52	—	—	—	—
	XJ1-184	3028.36	0.87	—	—	—	—
	XJ1-185	3030.17	1.07	—	—	—	—
	XJ1-186	3032.82	1.29	—	—	—	—
	XJ1-187	3034.64	2.84	—	—	—	—
	XJ1-188	3036.52	6.62	—	—	—	—
	XJ1-189	3038.39	2.15	—	—	—	—
	XJ1-190	3040.24	1.19	—	—	—	—
	XJ1-191	3042.24	17.74	—	—	—	—
	XJ1-192	3044.56	14.88	—	—	—	—
	XJ1-215	3046.18	2.57	—	—	—	—
	XJ1-216	3048.56	1.79	—	—	—	—
	XJ1-217	3050.37	2.57	—	—	—	—
	XJ1-218	3052.42	3.52	—	—	—	—
	XJ1-6	3055.49	1.33	0.75	28	11	6
	XJ1-8	3056.21	1.77	0.57	23	13	2
	XJ1-10	3057.56	0.81	0.61	21	16	2

Table 1. *Cont.*

Stratum	Sample No.	Depth (m)	TOC (%)	R_O (%)	Vitrinite (%)	Inertinite (%)	Exinite (%)
Taiyuan Formation	XJ1-28	3069.85	1.52	0.59	39	13	4
	XJ1-30	3071.45	1.27	0.69	23	14	3
	XJ1-37	3074.65	0.84	0.79	16	21	0
	XJ1-39	3075.9	1.85	0.56	14	22	3
	XJ1-47	3081.51	2.27	0.63	25	7	13
	XJ1-177	3083.56	2.56	0.62	29	6	0
	XJ1-178	3084.6	2.49	0.63	25	11	0
	XJ1-58	3089.75	0.95	0.61	17	16	5
	XJ1-66	3103.63	3.66	0.81	18	16	3
	XJ1-69	3105.35	1.39	0.85	24	18	3
	XJ1-76	3110.4	4.02	0.7	19	15	1
	XJ1-82	3113.08	5.19	0.59	17	18	0
	XJ1-153	3114.45	21.66	0.78	7	34	0
	XJ1-93	3116.1	11.25	0.79	18	19	1
	XJ1-98	3118.71	0.24	0.84	21	17	1
	XJ1-101	3119.9	0.47	0.75	19	21	0
	XJ1-171	3130.15	0.64	0.65	24	11	5
	XJ1-172	3131.4	9.21	0.37	21	12	5
	XJ1-M1	3088.50	—	0.67	53.2	35.3	8.7
	XJ1-M2	3107.05	—	0.62	40.1	46.4	0.6
	XJ1-M3	3109.85	—	0.59	70.1	17.6	6.0
	XJ1-M4	3117.30	—	0.70	52.0	33.9	4.2

The analysis of shale samples includes the detection of total organic carbon content (TOC), identification of kerogen macerals, and determination of vitrinite reflectance. The aforementioned analysis and testing are conducted in the laboratory of the Shandong Coal Geological Planning and Exploration Institute.

The determination of total organic carbon content is based on the method for determining total organic carbon in sedimentary rocks. The CS-230 carbon and sulfur analyzer (LECO, St. Jose, CA, USA) is utilized to analyze and test the samples in accordance with Chinese standards (GB/T19145-2022), and the accuracy was ±0.001–0.5% [34]; the process of identifying and categorizing kerogen and coal macerals through the use of transmitted light fluorescence is known as identification. In accordance with the Chinese standard experimental method SY/T5125-2014, 21 samples of shale and 4 samples of coal were analyzed, and the analysis results were subsequently utilized for kerogen-type identification [35]; the vitrinite reflectance of coal and shale samples was measured in accordance with the Chinese standard SY/T5124-2012 [36].

Based on the aforementioned experimental data, the organic matter maturity and hydrocarbon generation potential of shale in the Taiyuan Formation and Shanxi Formation were discussed using Origin (2021) software. This involved combining discriminant templates and analysis methods developed by previous researchers. Then, the geochemical data are combined with structural stratigraphic information collected from drilling data. The burial history, thermal evolution history, and hydrocarbon generation history of coal-bearing strata in Julu sag are simulated using PetroMod 1D (2012.2) software from Schlumberger.

3.2. Coal Seam

The coal-bearing strata in the study area are widely distributed within the Shanxi Formation and Taiyuan Formation. There are 8~17 coal-bearing layers in the strata, but only 4 stable and relatively mineable coal seams with a total thickness ranging from 5.44 m to 13.87 m.

The macroscopic coal rock types of the coal seams in the study area primarily consist of bright and semi-bright varieties. Microscopically, the main components of the coal are vitrinite, followed by inertinite, with exinite being present in the lowest concentration. The vitrinite is primarily composed of homogeneous vitrinite, followed by degradinite. The inertinite is mainly comprised of detrital inert, followed by fusinite, with a small presence of macrinite, microsomes, and sclerotinite. The exinite is primarily composed of microspores, followed by cutinite and a small amount of resinite. The mass fraction of vitrinite in coal ranges from 40.1% to 70.1%, with an average mass fraction of 53.85%. Additionally, the

mass fraction of inertinite is between 17.6% and 46.4%, with an average mass fraction of 33.3%. The mass fraction of the exinite is between 0.6% and 8.7%, with an average mass fraction of 4.88%.

3.3. Mud Shale

The composition of organic matter not only determines the gas generation potential of source rocks but also influences the micro-component characteristics, thereby affecting the occurrence pattern of coal-measure gas. Identifying the types of organic matter in coal-measure source rocks is crucial for understanding the mechanism of coal-measure gas accumulation. This holds great significance in academic research on this topic. The micro-components of coal rock–mud shale samples from Well XJ1 in the study area were analyzed, specifically focusing on the Taiyuan Formation–Shanxi Formation.

The results indicate that the organic matter in the Taiyuan–Shanxi Formation mud shale is predominantly classified as type II_2, with a small amount of type II_1 present. Additionally, only one sample exhibits type III kerogen (Figure 3). This suggests that the organic matter is primarily derived from lower aquatic phytoplankton. The analysis indicates that the source rocks of the Shanxi Formation–Taiyuan Formation exhibit a high potential for oil and gas generation.

The abundance of organic matter is a crucial parameter for assessing the quality of gas reservoirs. Analysis of the organic matter abundance data from Well XJ1 indicates that the total organic carbon (TOC) content of Shanxi Formation mud shale ranges from 0.81% to 17.74%, with an average value of 4.09%. The dominant source rocks are general in nature, followed by good- and high-quality source rocks. The total organic carbon (TOC) content of mud shale in the Taiyuan Formation ranges from 0.24% to 21.66%, with an average value of 3.97%. These mud shales are primarily composed of good- and high-quality source rocks, followed by general source rocks. This information suggests that the Taiyuan Formation contains a significant amount of favorable source rock for potential hydrocarbon generation (Figure 4b). The organic matter content in coal-measure shale ensures the potential for hydrocarbon generation and provides a guarantee of a gas source for the symbiotic accumulation of coal-measure gas. This is crucial for understanding the formation and extraction of coal-measure gas in academic research [37].

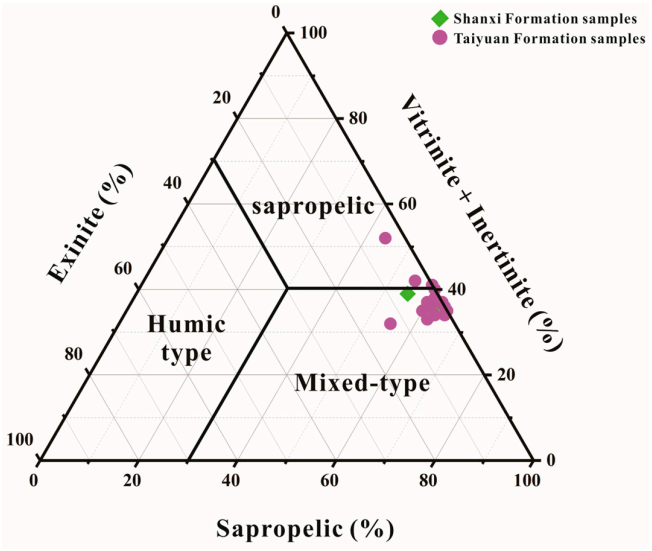

Figure 3. Triangular diagram of shale kerogen macerals in well XJ1 of Julu sag.

The maturity of organic matter is a crucial indicator for evaluating the hydrocarbon generation potential of coal mine reservoirs. This directly impacts gas generation as well as the occurrence, migration, and accumulation of gas after hydrocarbon generation. Therefore, understanding the maturity of organic matter can assist in determining the timing

of hydrocarbon generation and accumulation. This knowledge is crucial for assessing the potential for oil and gas formation. Analysis of vitrinite reflectance data collected from Well XJ1 and adjacent areas, as well as measured vitrinite reflectance of samples, indicates that the maturity (R_O) of shale in the Shanxi Formation at Well XJ1 falls within the range of 0.61% to 0.75%, with an average value of 0.64%. This places it in the immature–mature stage. The maturity (R_O) of shale in the Taiyuan Formation ranges from 0.37% to 0.91%, with an average of 0.66%, indicating that it is in the immature–mature stage (Figure 4a).

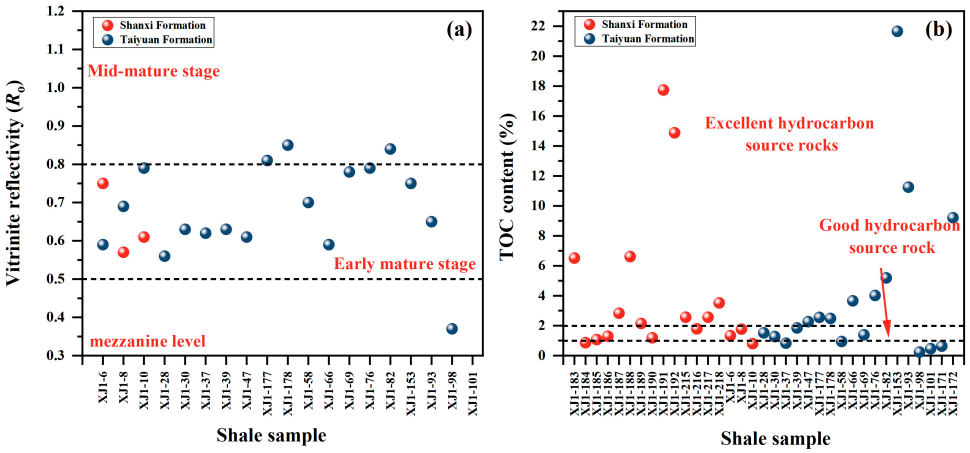

Figure 4. Scatter plot of shale samples from well XJ1 in Julu sag. (**a**) Maturity scatter diagram of shale samples; (**b**) the scatter diagram of organic matter content of shale samples.

4. Accumulation Process of Coal-Measure Gas

4.1. 1D Basin Modeling Method and Parameters

The data required for modeling and analysis of PetroMod 1D basin include the following parameters: strata, thickness, absolute age of sedimentary and erosion events, lithology, total organic carbon (TOC), hydrogen index (HI) value, and kinetic equation [38]. In addition, boundary conditions such as paleo-water depth, sediment–water interface temperature (SWIT), and paleo heat flow are utilized to constrain the modeling and analysis of one-dimensional basins [39]. The stratigraphic and structural data presented in this study are derived from the actual findings of the XJ1 well drilling. The determination of the absolute age of sedimentary and erosion events is based on previously published results [32,40–43]. Geochemical parameters such as total organic carbon (TOC) and hydrogen index (HI) values are determined through relevant experimental tests, as shown in Table 2.

Table 2. 1D basin modeling input data of XJ1 well in Julu sag.

Age (Ma)	Layer/Event	Depth (m)	Thickness (m)	Event Type	Paleodeposition /Erosion (m)	Lithology	PSE
5.33	N_2Y	829	398	Deposition		Shale and Sandstone	Overburden
17	N_1g	1227	403	Deposition		Shale and Sandstone	Overburden
66	E	1630	701	Erosion	800	Shale and Sandstone	Overburden
163.5	J_3-K_1	2331	0	Erosion	−100	Shale and Silt	Overburden
201.3	J_1-J_2	2331	0	Erosion	−1100	Sandstone	Overburden
251.9	T_1-T_2	2331	0	Erosion	−400	Sandstone	Overburden
254.14	P_2sh	2331	99	Deposition		Sandstone	Overburden
265.1	P_1x	2430	596	Deposition		Shale and Sandstone	Reservoir
296	P_1s	3026	37	Deposition		Sandstone (Clay Rich)	Reservoir
299	P_1s_2	3063	4	Deposition		Coal	Source Rock
303	C_3t_1	3067	6	Deposition		Coal	Source Rock
303.5	C_3t_2	3073	58	Deposition		Shale (Organic Rich, 3% TOC)	Reservoir
307	C_3b	3131	239	Deposition		Dolomite (typical)	Reservoir

The paleo heat flow value in the study area is determined through the tectonic evolution process. By integrating previous research findings and employing the EASY % RO model, we have made predictions regarding the heat flow value. The calculation formula is as follows:

$$R_O\ \% = \varphi\ (\Delta v, t) \quad (1)$$

$$Q = kdT/dZ \quad (2)$$

Among these variables, v represents the heating rate, t denotes the heating time, Q signifies the heat flow value, k stands for rock thermal conductivity, and dT/dZ indicates the geothermal gradient. Combining Equations (1) and (2), the expression for R_O as a function of Q, Z, and T can be derived. The calculation formula is as follows:

$$R_O\ \% = \psi\ (Q, Z, t) \quad (3)$$

In the analysis of basin modeling, various heat flow values from predecessors are used as input to create an optimal basin model. The heat flow value is then optimized based on the measured Ro value, resulting in the best fitting outcome. The ancient water depth value is determined based on the previous analysis of the sedimentary environment in the study area, which falls within the 39°~40° zone of East Asia in the Northern Hemisphere. The surface temperature of sedimentary water (SWIT) is automatically determined using the PetroMod (2012.2) software.

4.2. Numerical Simulation of the Hydrocarbon Generation Process

Based on the numerical simulation results of the burial history, it is evident that the coal-measure strata in the study area have undergone two distinct processes: initial slow deposition, rapid subsidence, and burial, followed by significant uplift and denudation (Figure 5). These findings are presented as follows:

(1) From the Late Carboniferous to the Early Triassic, the North China platform began to disintegrate under the influence of the Indosinian movement. This disintegration was a result of the scissors collision between the North China Plate and the Yangtze Plate from east to west, leading it into a development stage of the continental margin active zone.

The entire North China region experienced uplift, leading to the development of the Julu sag and its interaction with the sea–land interface. This process resulted in the gradual deposition of Carboniferous and Permian strata [32]. Among them, the rate of formation deposition is approximately 21 m/Ma, and the burial depth is relatively shallow. In the early Triassic, the study area essentially retained the paleogeographical pattern of the Late Permian. Due to the increased compressive stress in the northern and southern regions of the North China Plate, there has been a continued uplift of the plate and a reduction in the size of the basin, leading to the development of large inland depressions. At this time, the strong uplift in the northern part of the North China Plate led to the formation of a paleo-topography with high elevation in the north and low elevation in the south. This uplift also provided abundant sediment sources for the North China Basin. During this period, the deposition rates at the two ends and the center of the basin exhibited variations, leading to the rapid deposition of Triassic strata. The subsidence rate was recorded at 57 m/Ma, resulting in a burial depth of 2000 m.

(2) From the Early Triassic to the end of the period, due to the early activities of the Yanshan cycle, there was a significant scissor-type collision and splicing of the Yangtze plate and the North China plate from east to west. This led to a climax in which most of North China experienced uplift and denudation [41]. During this period, due to the influence of the Yanshan movement, there was a significant uplift of the strata and extensive erosion of the Triassic strata. The estimated uplift rate during this period was approximately 22 m per million years (Ma).

(3) From the Early Jurassic to the Middle Cretaceous, during the middle stage of the Yanshan cycle in the Jurassic period, the activity of the western Pacific plate emerged as the primary controlling factor for the evolution of eastern basins in my country. At

this stage, the Linqing Depression was controlled by NE-NNE and NW-NWW trending faults. The study area experienced tension and subsidence, although the subsidence was relatively weak. During this period, detrital rocks of Middle-Lower Jurassic and coal-bearing clastic rocks were formed in the basin [42]. The deposition rate of the thin layer in the sedimentary stratum is approximately 13 m per million years (m/Ma). During the Late Jurassic to Middle Cretaceous period, the Yanshan movement caused the activation of the Lanliao fault in the east of the Linqing Depression and the Maling fault in the south. This movement also controlled the deposition of sediments from the Upper Jurassic to Lower Cretaceous periods. However, it is important to note that, despite these changes, the overall tectonic setting from the Early to Middle Jurassic periods remains preserved. Furthermore, the extensional action in the study area led to an increase in subsidence, resulting in the continued development of clastic rock and coal-bearing clastic rock deposits within the basin. At this stage, the deposition rate of the formation was approximately 21 m per million years, and the burial depth reached its maximum during the Middle Cretaceous period.

(4) During the Middle Cretaceous to the Late Cretaceous, the study area underwent two distinct stages: the Late Yanshan cycle and the Early Himalayan cycle. The Yanshan cycle, which occurred later, further intensified the activity of the eastern part of the North China Plate. This led to continued crustal uplift and erosion of the Cretaceous sedimentary strata. During the Early Paleogene, due to the early influence of the Himalayan cycle, there was further uplift of the crust, leading to the denudation of all Mesozoic strata. The maximum uplift during this period was 1800 m, with a strata uplift rate of approximately 52 m/Ma.

(5) During the Paleogene to Neogene periods, there was a noticeable development of rifted basins in the study area due to the intensified Himalayan tectonic movements. A significant number of new faults were generated as a result of Cenozoic rifting. Additionally, substantial deposits of thick Paleogene material accumulated in the western Qiuxian sag and Nangong sag. Furthermore, the formation of the Guantao and Tangyi uplifts also commenced during this period [43]. During this stage in the study area, the Paleogene strata were deposited at a rate of approximately 17 m/Ma. During the early Neogene period, the North China Plate underwent significant sedimentary and tectonic changes in the western Linqing Depression due to the influence of the Himalayan movement. This resulted in a distinct "north-south division and an east-west division" in its sedimentary characteristics and tectonic pattern. During this time period, the study area underwent a slight uplift, with the denuded strata reaching a thickness of approximately 100 m. The rate of stratum uplift was estimated to be around 17 m per million years (Ma). Later, the entire study area is characterized by regional subsidence and has been receiving deposits since the Cenozoic era. The deposition rate of the stratum is estimated to be approximately 68 m per million years (Ma).

Based on the simulation results for the thermal evolution history (Figure 6), it is evident that the hydrocarbon generation evolution history of coal source rocks in the study area can be categorized into three stages. The first stage is characterized by protist biogenic gas generation before the Mesozoic and Early Cretaceous. This is followed by primary hydrocarbon generation from the Mesozoic Early Cretaceous to the Late Cretaceous, and finally, the secondary hydrocarbon generation stage since the late Cenozoic. The specific process is outlined as follows:

From the Late Carboniferous to the early Late Cretaceous, the paleotemperature in this area remained relatively stable, exhibiting a geothermal gradient of approximately 3.2~3.7 °C/100 m. From the Late Carboniferous to the Early Triassic, the source rock strata gradually subsided, leading to a continuous increase in burial depth, eventually reaching 1600 m (Figure 6). Due to the influence of epigenetic metamorphism, the coal-measure source rock was heated up, reaching a temperature of 65 °C. As a result, $R_{O,\,max}$ increased slowly. By the end of the Early Triassic, the maximum vitrinite reflectance ($R_{O,\,max}$) of coal-measure source rocks reached 0.4% but did not exceed the threshold for oil generation (Figure 7).

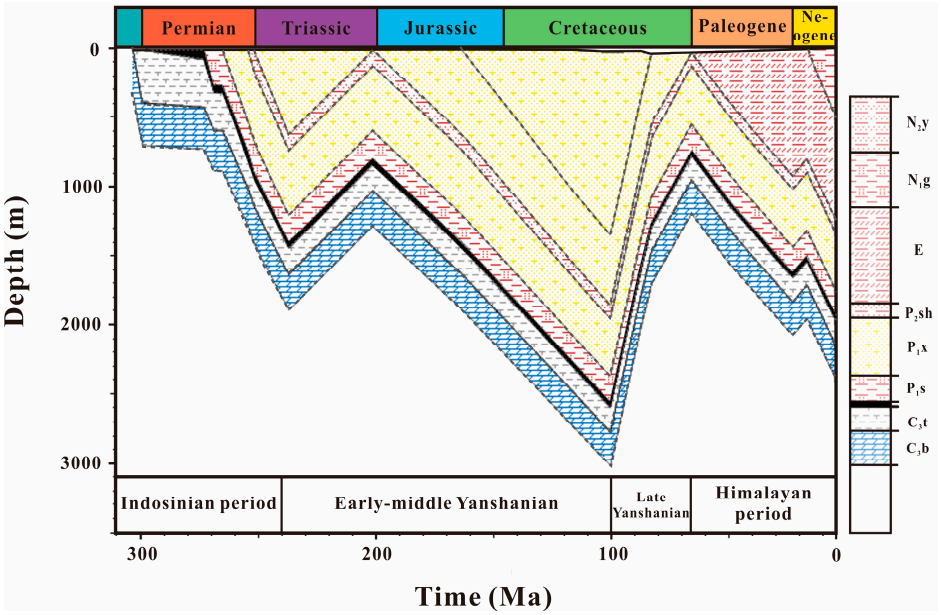

Figure 5. Sedimentary-burial history of Julu study area.

At this stage, hydrocarbon generation is primarily derived from biogenic gas. The coal rock exhibits a low degree of metamorphism and is currently in the soft lignite stage. From the Middle Triassic to the end of the Late Triassic, as a result of the early Yanshan movement, the strata experienced uplift and denudation, leading to the cessation of hydrocarbon generation (Figure 6). During the Early Jurassic to the Middle Cretaceous, the coal-measure source rocks in the study area underwent sedimentation and burial influenced by the Yanshan tectonic movement. It is noted that these rocks reached a maximum burial depth of approximately 2750 m (Figure 6). Affected by the deep geothermal field, the coal and rock are heated to temperatures reaching up to 90 °C. As a result, $R_{O,max}$ reaches 0.50%, leading to a transformation in the quality of the coal into long-flame coal. At this stage, primary hydrocarbon generation occurs, leading to the accumulation of a significant amount of coalbed methane. From the Middle Cretaceous to the Early Paleogene, the study area was under the influence of the Yanshan cycle, leading to tectonic control and significant uplifting and denudation. These processes continued until the end of the Yanshan tectonic cycle. The effective bedrock thickness above the gas reservoir is less than 400 m. The caprock of coalbed methane has been severely damaged, leading to a halt in hydrocarbon generation. Additionally, the Yanshan movement has resulted in numerous NNE-trending extensional faults, causing the previously formed coal and gas to escape rapidly [1] (Figure 6). Since the Paleogene period, magmatic activity has intensified due to the influence of the Himalayan tectonic movement. As a result, the coal source rocks have entered an abnormally high temperature stage (Figure 6). The geothermal gradient increased to approximately 6.2 °C/m, with the highest recorded temperature reaching about 110 °C. Additionally, $R_{O,max}$ experienced another increase, rising to 0.8% (Figure 7). Thermogenic gas was the dominant factor, leading to the coal rocks entering the long-flame coal stage and reaching the second peak of hydrocarbon generation. During this stage, the coal-measure source rocks were undergoing sedimentation and burial processes. However, the majority of these layers are thick deposits in fluvial facies, which are not conducive to the preservation of coalbed methane (Figures 7 and 8). Regional tectonic burial has resulted in the current coal-measure gas being characterized by "significant burial depth and low gas content" [1].

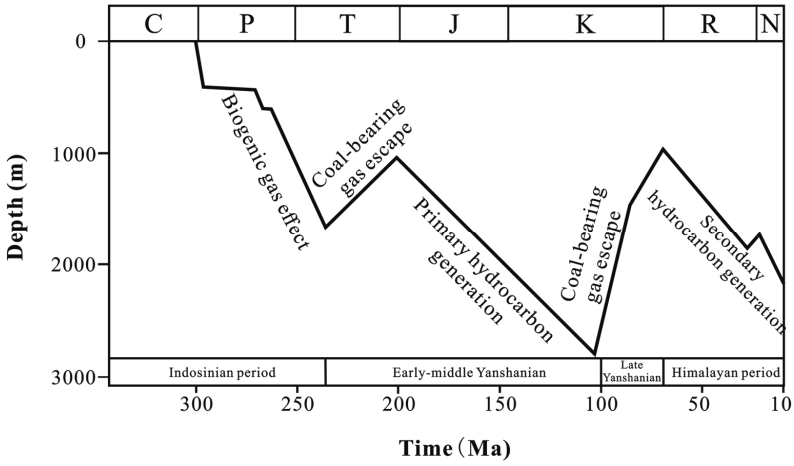

Figure 6. Hydrocarbon generation and the evolutionary history of source rocks in the study area.

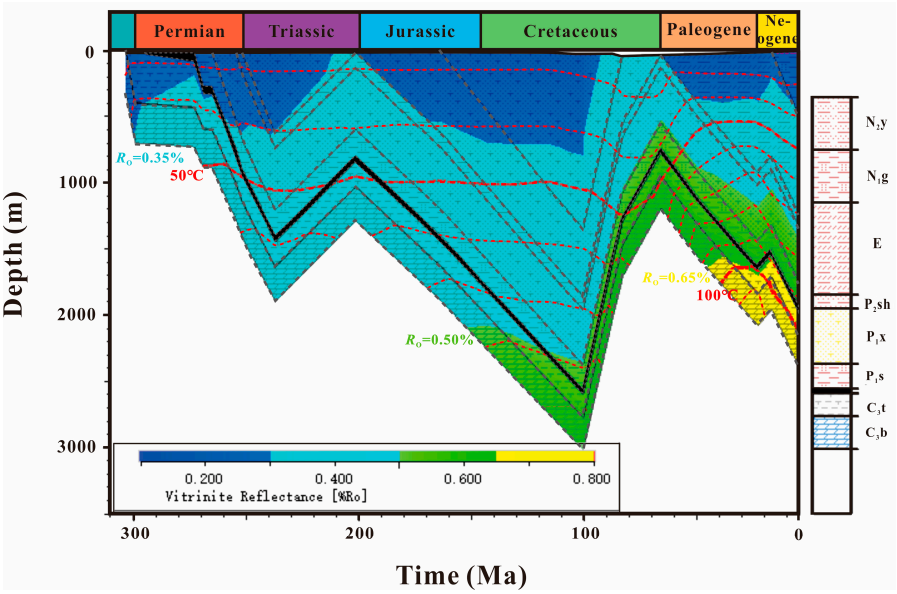

Figure 7. Evolution of sedimentary burial and hydrocarbon generation history in the study area.

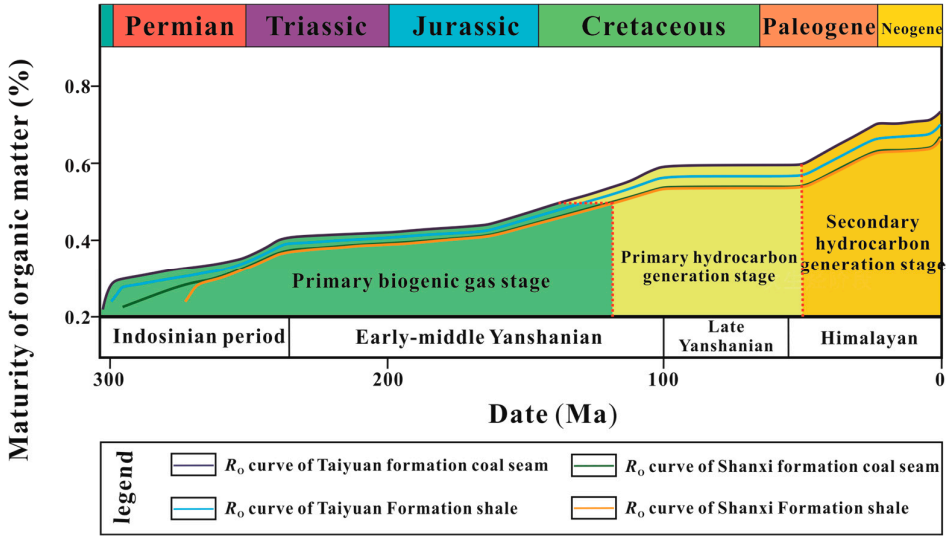

Figure 8. Evolutionary history of organic matter maturity in the study area.

4.3. Analysis of the Accumulation Process

The source rocks in the study area are primarily situated in the middle and lower sections of the Shanxi Formation, as well as the lower portion of the Taiyuan Formation. Both coal seams and mud shale serve as the primary source rocks within this region. In the study area, there are three different sealing modes of coal-measure gas caprocks: mutual caprocks consisting of coal and mudstone, sandstone serving as the caprock for the coal seam, and sandstone acting as the caprock for the mudstone (Figure 9).

Coal and mudstone act as caprocks for each other. Coal seams, serving as caprocks, exhibit a superior capacity for hydrocarbon generation, while the hydrocarbon-generating capacity of mudstone is weaker in comparison to that of coal seams. The natural gas produced by coal seams serves to provide concentration sealing and pressure sealing for the natural gas produced by mudstone, thereby preserving the natural gas in coal measures. Mud shale, as the cover of coal seams, exhibits low porosity and permeability, making it difficult for the natural gas produced by coal seams to diffuse upward, resulting in a sealing effect. Coal and mudstone are considered to be the mutual caprock models. This model allows for the easy preservation of natural gas in coal measures, as well as a relatively high gas content within the reservoir [4].

Sandstone, as the direct caprock of coal seams and mud shale, exhibits better porosity and permeability conditions. In contrast, coal seams and mud shale possess superior hydrocarbon-generating capacity. Sandstone does not provide optimal sealing conditions, but it does offer excellent storage space. It can serve as an effective reservoir rock for retaining natural gas that escapes from coal seams and mud shale, thereby forming tight sandstone gas reservoirs.

Based on the simulation results of the structure-burial history, thermal evolution history, and hydrocarbon generation history in the area, it is determined that the coal-measure source rock reached its maximum burial depth during the Middle Cretaceous period and subsequently entered into the first peak of hydrocarbon generation. However, due to the influence of the Yanshan tectonic cycle, the stratum experienced uplift and denudation. This led to a suspension in the hydrocarbon generation stage of the coal-measure source rock, resulting in shallower burial depths and deteriorating sealing conditions. Consequently, this has caused the escape of coal-measure natural gas. Since the Paleogene, there has been an increase in the burial depth of coal-measure source rocks. This has led to the rapid maturation of these rocks under the influence of magma heat, resulting in a secondary hydrocarbon generation process and the production of a significant amount of oil and gas.

In comparison with the southern Qinshui Basin, where CBM development is more active than in the study area (Table 3), the coal seam thickness of the Shanxi–Taiyuan Formation in the Julu Sag is relatively thin, and the burial depth of the coal seam is significantly greater. Through on-site analysis of coal samples in the study area, it was found that the gas content of each coal seam sample is less than 1 m^3/t. According to the "Coalbed Methane Reserve Estimation Specification" (DZ/T0216-2020) [44], if the gas content of the coalbed air drying base is not less than 4 m^3/t, then the lower limit of the coalbed methane resource budget indicates that CBM in the study area has no development value [45,46].

The Shanxi–Taiyuan Formation mudstone in the study area is widely distributed, thick, and stable. The Shanxi Formation exhibits a medium total organic carbon (TOC) content and possesses good potential for hydrocarbon generation. The composition of the source rocks is primarily general, with some being good-quality and some being high-quality source rocks. However, these rocks have poor porosity and permeability (Table 3). The reservoir is characterized by ultra-low porosity and ultra-low permeability, making it unfavorable for the seepage of shale gas (Table 3). However, the Taiyuan Formation exhibits a high total organic carbon (TOC) content and possesses significant hydrocarbon generation potential. It primarily consists of high-quality source rocks with low porosity and permeability. The Shanxi–Taiyuan shale reservoir is characterized by ultra-low porosity and ultra-low permeability, making it unfavorable for the seepage of shale gas. However,

this particular shale formation has a low clay mineral content and a high concentration of brittle minerals such as quartz. This composition is advantageous for enhancing and transforming the reservoir.

In general, the coal seam in the study area is deeply buried, thin in thickness, and low in gas content. It is difficult to develop a single coalbed methane source, and the economic benefit is low. In comparison, the coal-measure source rock mud shale in the study area is thicker, has a higher organic matter content, and has great hydrocarbon-generating potential, which can effectively provide a gas source guarantee for coal-measure gas symbiotic reservoirs and provide a material basis for independent coal-measure gas reserves at the same time. In addition, mudstone and siltstone of the Lower Shihezi Formation with tens to hundreds of meters are widely developed in the upper part of the source rock in the whole study area, which is a good caprock and reservoir rock of the coal-measure source rock in the study area and constitutes a favorable source-reservoir caprock. The combination is not only conducive to the generation of coalbed methane and shale gas, but also provides a large amount of storage space to form tight sandstone gas reservoirs.

The coalbed methane, shale gas, and tight sandstone gas in the study area are spatially superimposed multiple times. Under the mechanism of symbiotic regulation, they form a unified energy system as a whole, and the differences in accumulation are expressed as a distinct sub-level energy system. Furthermore, the clay mineral content in the reservoir within the study area is relatively low, while the presence of brittle minerals such as quartz is notably high. This characteristic proves advantageous for the exploration and development of coal-measure "three gas" resources in later stages.

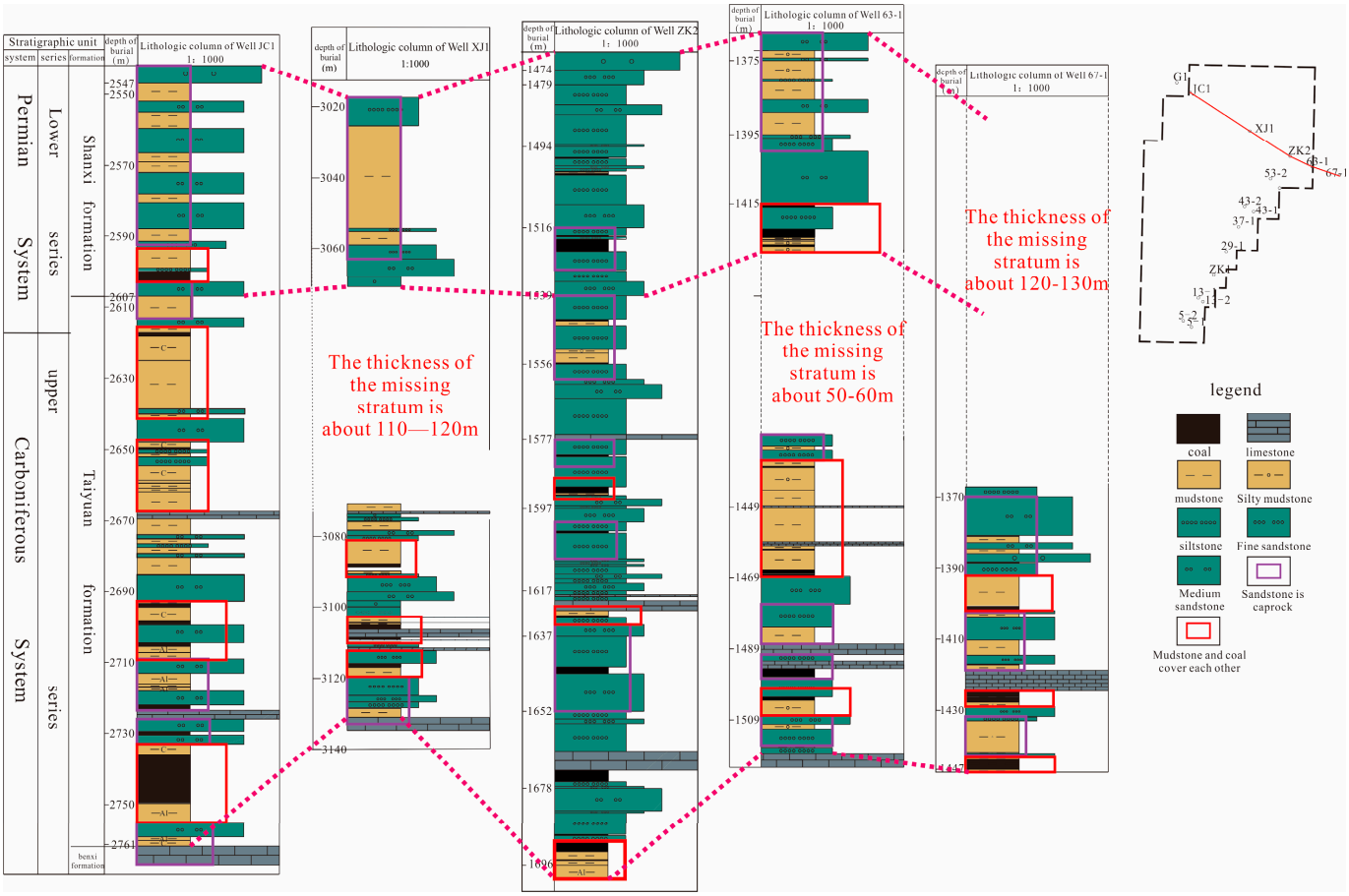

Figure 9. Distribution characteristics of source rocks in Julu Sag within the Shanxi–Taiyuan Formation coal measures.

Table 3. Comparison of coal (rock) layer characteristics between the southern Qinshui Basin and Julu Sag.

Coal (Rock) Layer Characteristics		Coal-Bearing Basin			
		Southern Qinshui Basin		Julu Sag	
Coal seam	Series of strata	Shanxi Formation (No. 3 coal)	Taiyuan Formation (No. 15 coal)	Shanxi Formation (No. 2 coal)	Taiyuan Formation (No. 8 coal)
	Buried depth (m)	208.0–1150.0	208.0–1121.3	1300–3060	1580–3100
	Thickness (m)	0.50 [(a)]–11.2 [(b)] (6.0) [(c)]	0.4 [(a)]–19.4 [(b)] (6.4)	2.34 [(a)]–5.80 [(b)] (4.02)	1.57 [(a)]–3.23 [(b)] (2.44)
	Porosity (%)	0.63 [(a)]–10.59 [(b)]	0.63 [(a)]–10.59 [(b)]	—	—
	Permeability (mD)	0.004 [(a)]–13.010 [(b)] (1.570) [(c)]	0.010 [(a)]–6.640 [(b)] (1.130) [(c)]	—	—
	Gas content ($m^3 \cdot t^{-1}$)	3.7 [(a)]–27.4 [(b)] (13.8) [(c)]	6.6 [(a)]–35.1 [(b)] (17.4) [(c)]	0.25 [(a)]–1.93 [(b)] (0.733) [(c)]	0.22 [(a)]–1.01 [(b)] (0.53) [(c)]
Mudstone	Thickness (m)	16.00 [(a)]–90.0 [(b)] (30.0) [(c)]	10.0 [(a)]–60.0 [(b)] (35.0) [(c)]	80 [(a)]–100 [(b)] (90) [(c)]	20 [(a)]–50 [(b)] (30) [(c)]
	Porosity (%)	2.15 [(a)]–6.95 [(b)] (4.22) [(c)]	2.35 [(a)]–5.46 [(b)] (4.28) [(c)]	6.44	1.31 [(a)]–4.99 [(b)] (2.59) [(c)]
	Permeability (mD)	—	—	0.00196	0.000278 [(a)]–0.0529 [(b)] (0.00863) [(c)]
	TOC (%)	0.43 [(a)]–6.42 [(b)] (2.07) [(c)]	0.36 [(a)]–3.94 [(b)] (1.89) [(c)]	0.81 [(a)]–17.74 [(b)] (4.09) [(c)]	0.24 [(a)]–21.66 [(b)] (3.97) [(c)]
	Hydrocarbon potential ($mg \cdot g^{-1}$)	0.99	0.99	0.69 [(a)]–82.07 [(b)] (15.75) [(c)]	0.46 [(a)]–130.44 [(b)] (22.19) [(c)]
	Composition of mineral	Clay mineral content is 50.0–63.0% with an average of 58.0%	Clay mineral content is 53.0–62.0% with an average of 56.6%	Clay mineral content is 26.6–56.0% with an average of 46.1%, followed by quartz, with content between 21.0 and 37.5%	Clay mineral content is 24.4–70.5% with an average of 44.5%, followed by quartz, with content between 23.4 and 64.5%

[(a)] Maximum; [(b)] minimum; [(c)] average.

5. Conclusions

The predominant source rocks in the study area consist mainly of coal and shale, ranging from the Shanxi formation to the Taiyuan formation. Among the micro-components, vitrinite has the highest content, followed by inertinite, and exinite has the lowest content. The organic matter present is predominantly type II_2, with a high abundance of organic material primarily in the low to mature stage. It exhibits good hydrocarbon generation potential, indicating that the source rock is of good quality.

The tectonic-burial history of the study area can be divided into three main phases. The first phase is characterized by a primitive, slow deposition process in the lower Paleozoic. This was followed by a rapid subsidence and burial process, as well as massive uplift and denudation processes in the Mesozoic. The final phase involved rapid subsidence and burial processes with small-scale structural uplift since the Cenozoic.

The hydrocarbon generation and evolution history of coal-measure source rocks in the study area can be categorized into three stages. Firstly, there is the protist biogenic gas stage before the Mesozoic and the Early Cretaceous. This is followed by the primary hydrocarbon generation process caused by rapid burial at the end of the Mesozoic, Early Cretaceous, and Late Cretaceous. Finally, there is the secondary hydrocarbon generation stage of thermal anomalies since the late Cenozoic. In general, the secondary generation of hydrocarbons plays a crucial role in the accumulation of natural gas in regional coal mines.

In the study area, there are three different sealing modes of coal-measure natural gas caprocks: mutual caprocks of coal and mudstone, sandstone as the caprock of coal seams, and sandstone as the caprock of mudstone. Under varying capping conditions, different levels of hydrocarbon-generating potential and coal-measure gas reservoirs are formed. Among these, coal-measure natural gas is easily preserved in the model of coal and mudstone as caprocks, with a high gas content in the reservoir. Sandstone, serving as a

caprock model, can effectively preserve natural gas escaping from coal seams and shale, thus forming tight sandstone gas reservoirs that serve as good reservoir rocks.

The hydrocarbon-generating capacity of different coal-measure source rocks varies, and coal plays a crucial role in coalbed methane reservoirs. However, in the study area, the coal seam thickness is relatively thin and buried deep. Additionally, the gas content is low, and, as a result, the coalbed methane reservoir has minimal impact on the overall richness of coalbed methane in this particular area of study. Organic matter-rich shale plays a crucial role in coal-measure natural gas reservoirs. In the study area, the Shanxi Formation–Taiyuan Formation mudstone exhibits high organic matter abundance, significant thickness, and substantial hydrocarbon generation potential. These characteristics effectively ensure a gas source for co-generating coal-measure gas reservoirs and provide a material basis for the formation of independent coal-measure shale gas reservoirs simultaneously. The sandstone caprock in the study area not only provides effective storage space but also serves as a geological basis for the accumulation of coal-measure tight sandstone gas.

Author Contributions: Conceptualization, Y.W. and H.Z.; methodology, Y.W.; software, Y.W., H.Z. and L.Y.; validation, Y.W., H.Z. and L.Y.; formal analysis, Y.W. and H.Z.; investigation, Y.W.; resources, H.Z.; data curation, H.Z.; writing—original draft preparation, Y.W.; writing—review and editing, Y.W., H.Z., L.Y., Y.Z. and Z.C.; visualization, H.Z.; supervision, Y.W.; project administration, L.Y.; funding acquisition, Y.W. All authors have read and agreed to the published version of the manuscript.

Funding: This research was funded by the National Natural Science Foundation of China (42172156, 41802183) and the Fundamental Research Funds for the Central Universities (2022YCPY0201).

Data Availability Statement: Data are contained within this article.

Acknowledgments: We would like to thank the Key Laboratory of Coalbed Methane Resources and Reservoir Formation Process for all the support provided in this research.

Conflicts of Interest: The authors declare that they have no known competing financial interests or personal relationships that could have appeared to influence the work reported in this paper.

References

1. Xie, W.D.; Wang, M.; Hou, X.W. Study on enrichment zones and enrichment regularity of coalbed methane in Hebei province. *J. Henan Polytech. Univ. Nat. Sci.* **2018**, *37*, 17–25. (In Chinese)
2. Jiang, T.; Liu, Z.Y.; Wang, T.; Song, H.Z. Discussion on Upper Paleozoic Coal Measures Gas Reservoiring Mechanism in Northeastern Ordos Basin. *Coal. Geol. China* **2015**, *27*, 43–47. (In Chinese)
3. Cao, D.Y.; Yao, Z.; Li, J. Evaluation Status and Development Trend of Unconventional Gas in Coal Measure. *Coal Sci. Technol.* **2014**, *42*, 89–92. (In Chinese)
4. Zhu, Y.M.; Hou, X.W.; Cui, Z.B.; Liu, G. Resources and reservoir formation of unconventional gas in coal measure, Hebei Province. *J. China Coal Soc.* **2016**, *41*, 202–211.
5. Cao, Y.T.; Liu, L.; Chen, D.L.; Wang, C.; Yang, W.Q.; Kang, L.; Zhu, X.H. Partial melting during exhumation of Paleozoic ret–rograde eclogite in North Qaidam, western China. *J. Asian Earth Sci.* **2017**, *148*, 223–240. [CrossRef]
6. Feng, Z.J.; Dong, D.Z.; Tian, J.Q.; Qiu, Z.; Wu, W.; Zhang, C. Geochemical characteristics of longmaxi formation shale gas in the weiyuan area, Sichuan Basin, China. *J. Petrol. Sci. Eng.* **2018**, *167*, 538–548. [CrossRef]
7. Wang, Z.; Zhao, J.Z.; Chen, Y.H. Analysis of palaeo–sedimentary environment and characteristics of Shanxi formation in Shenfu area on the eastern margin of Ordos basin. *J. Xi'an Shiyou Univ. Nat. Sci. Ed.* **2019**, *34*, 24–30. (In Chinese)
8. Sang, S.X.; Han, S.J.; Liu, S.Q.; Zhou, X.Z.; Li, M.X.; Hu, Q.J.; Zhang, C. Comprehensive study on the enrichment mechanism of coal bed methane in high rank coal reservoirs. *J. China Coal Soc.* **2022**, *47*, 388–403. (In Chinese)
9. Gao, J.; Li, X.S.; Cheng, G.X.; Luo, H.; Zhu, H.J. Structural evolution and char-acterization of organic-rich shale from macroscopic to microscopic resolution: The significance of tectonic activity. *Adv. Geo-Energy Res.* **2023**, *10*, 84–90. [CrossRef]
10. Zhu, H.J.; Huang, C.; Ju, Y.W.; Bu, H.L.; Li, X.S.; Yang, M.P.; Chu, Q.Z.; Feng, H.Y.; Qiao, P.; Qi, Y.; et al. Multi-scale multi-dimensional characterization of clay-hosted pore networks of shale using FIBSEM, TEM, and X-ray micro-tomography: Implications for methane storage and migration. *Appl. Clay Sci.* **2021**, *213*, 106239. [CrossRef]
11. Cao, D.Y.; Liu, K.; Liu, J.C.; Xu, H.; Li, J.; Qin, G.H. Combination characteristics of unconventional gas in coal measure in the west margin of Ordos Basin. *J. China Coal Soc.* **2016**, *41*, 277–285. (In Chinese)
12. Qin, Y.; Shen, J.; Shen, Y.L. Joint mining compatibility of superposed gas–bearing systems: A general geological problem for extraction of three natural gases and deep CBM in coal series. *J. China Coal Soc.* **2016**, *41*, 14–23. (In Chinese)

13. Liang, B.; Shi, Y.S.; Sun, W.J.; Liu, Q. Reservoir forming characteristics of "the three gases" in coal measure and the possibility of commingling in China. *J. China Coal Soc.* **2016**, *41*, 167–173. (In Chinese)
14. Zhong, J.H.; Liu, C.; Wu, J.G.; Zhang, S.R.; Yang, G.Q. Symbiotic accumulation characteristics of coal measure gas in Linxing Block, eastern Ordos Basin. *J. China Coal Soc.* **2018**, *43*, 1517–1525. (In Chinese)
15. Zhang, Q.X.; Li, P.; Niu, F.; Li, X.W.; Yang, B.; Yan, H.Q. Accumulation characteristics of coal measures gas and its symbiosis combination models in Hanxing area of Hebei Province. *Sci. Technol. Eng.* **2021**, *21*, 4811–4820. (In Chinese)
16. Zheng, C.; Ma, D.M.; Xia, Y.C.; Chen, Y.; Li, W.B. Development mode and tectonic control of CBM enrichment in Hancheng Mlining Area. *Coal Eng.* **2021**, *53*, 89–94. (In Chinese)
17. Yu, K.; Ju, Y.W.; Qi, Y.; Huang, C.; Zhu, H.J. Geological process of Late Paleo-zoic shale gas generation in the eastern Ordos Basin, China: Revelations from ge-ochemistry and basin modeling. *Int. J. Coal Geol.* **2020**, *229*, 103569. [CrossRef]
18. Cox, I.A.; Pashin, J.C. Burial and thermal history modeling of basins in convergent oblique-slip mobile zones: A case study of the Ardmore Basin, southern Oklahoma. *Int. J. Coal Geol.* **2024**, *285*, 104486. [CrossRef]
19. Reda, M.; Abdel-Fattah, M.I.; Fathy, M.; Bakr, A. Integrated analysis of source rock evaluation and basin modelling in the Abu Gharadig Basin, Western Desert, Egypt: Insights from pyrolysis data, burial history, and trap characteristics. *Geol. J.* **2024**, *59*, 1416–1443. [CrossRef]
20. Li, Z.Y.; Gou, H.G.; Xu, X.F.; Li, X.; Miao, K.; Zhang, J.; Li, Z.G.; Li, Z.M.; Yang, W. Petroleum System Analysis and Burial History of Middle Permian Source Rock in Turpan–Hami Basin, NW China. *Minerals* **2024**, *14*, 347. [CrossRef]
21. Liu, P.; Zhang, T.Q.; Xu, C.; Wang, X.F.; Liu, C.J.; Guo, R.L.; Lin, H.F.; Yan, M.; Qin, L.; Li, Y. Organic matter inputs and depositional palaeoenvironment recorded by biomarkers of marine–terrestrial transitional shale in the Southern North China Basin. *Geol. J.* **2022**, *57*, 1617–1627. [CrossRef]
22. Nie, H.K.; Chen, Q.; Li, P.; Dang, W.; Zhang, J.C. Shale gas potential of Ordovician marine Pingliang shale and Carboniferous–Permian transitional Taiyuan–Shanxi shales in the Ordos Basin, China. *Aust. J. Earth Sci.* **2023**, *70*, 411–422. [CrossRef]
23. Lash, G.G.; Blood, D.R. Organic matter accumulation, redox, and diagenetic history of the Marcellus Formation, southwestern Pennsylvania, Appalachian basin. *Mar. Petrol. Geol.* **2014**, *57*, 244–263. [CrossRef]
24. Wang, M.J.; Zhang, X.H.; Zhang, Y.B.; Li, W.T.; He, D.F.; Sun, Y.P. Accumulation conditions of Upper Palaeozoic coal–derived gas in Eastern Linqing Depression. *Energ. Explor. Exploit.* **2013**, *31*, 31–56. [CrossRef]
25. Liu, Q.Y.; He, L.J.; Huang, F.; Zhang, L.Y. Cenozoic lithospheric evolution of the Bohai Bay Basin, eastern North China Craton: Constraint from tectono–thermal modeling. *J. Asian Earth Sci.* **2016**, *115*, 368–382. [CrossRef]
26. Xu, W.; Li, Y.; Cheng, L.Y. Meso-Cenozoic rheological structure of the Linqing Depression: Implications for cratonic destruction. *Geol. J.* **2021**, *56*, 1281–1290. [CrossRef]
27. Zhang, H.Y.; Wang, Y.; Chen, H.R.; Zhu, Y.M.; Yang, J.H.; Zhang, Y.S.; Dou, K.L.; Wang, Z.X. Study on Sedimentary Environment and Organic Matter Enrichment Model of Carboniferous–Permian Marine–Continental Transitional Shale in Northern Margin of North China Basin. *Energies* **2024**, *17*, 1780. [CrossRef]
28. Li, Y.; Zhao, L.Y.; Wang, X.B.; Huang, X.L.; Zhang, H.; Cui, K.; Dou, F.K. Analysis of Coal Measures Argillutite Hydrocarbon Generation Conditions—A Case Study of Upper Paleozoic Group in Eastern Linqing Depression. *Coal. Geol. China* **2016**, *28*, 12–17. (In Chinese)
29. Qi, J.F.; Yang, Q. Cenozoic structural deformation and dynamic processes of the Bohai Bay basin province, China. *Mar. Petrol. Geol.* **2010**, *27*, 757–771. [CrossRef]
30. Yu, K.; Ju, Y.W.; Qian, J.; Qu, Z.H.; Shao, C.J.; Yu, K.L.; Shi, Y. Burial and thermal evolution of coal–bearing strata and its mechanisms in the southern North China Basin since the late Paleozoic. *Int. J. Coal Geol.* **2018**, *198*, 100–115. [CrossRef]
31. Guo, H.; Xia, B.; Chen, G.W.; Wang, R.H.; Ding, J.H.; Wang, J.J. Geochemical and geotectonic features of Miocene basalts in Linqing Sag. *Acta Pet. Sin.* **2005**, *26*, 5–11. (In Chinese)
32. Lyu, X.Y.; Jiang, Y.L.; Liu, J.D.; Xu, T.W. Geochemical characteristics and hydrocarbon generation potential of the first member of Shahejie Formation (E2s1) source rocks in the Dongpu Depression, East China. *Geol. J.* **2019**, *54*, 2034–2047. [CrossRef]
33. He, J.H.; Ding, W.L.; Jiang, Z.X.; Li, A.; Wang, R.Y.; Sun, Y.X. Logging identification and characteristic analysis of the lacustrine organic–rich shale lithofacies: A case study from the Es3L shale in the Jiyang Depression, Bohai Bay Basin, Eastern China. *J. Petrol. Sci. Eng.* **2016**, *145*, 238–255. [CrossRef]
34. *GB/T19145-2022*; Determination for Total Organic Carbon in Sedimentary Rock. China Standard Press: Beijing, China, 2022.
35. *SY/T5125-2014*; Method of Identification Microscopically the Macerals of Kerogen and Indivision the Kerogen Type by Transmitted-Light and Fluorescence. China Standard Press: Beijing, China, 2014.
36. *SY/T5124-2012*; Method of Determining Microscopically the Reflectance of Vitrinite in Sedimentary. China Research Institute of Petroleum Exploration and Development: Beijing, China, 2012.
37. Sun, Y.T.; Xu, S.Y.; Zhang, S.Q.; Li, Y.L.; Li, H.; Meng, T.; Liu, J. Evolution of the Mesozoic source rocks in the West Linqing Depression. *Nat. Gas Geosci.* **2015**, *26*, 1910–1916.
38. Büker, C.; Littke, R.; Welte, D.H. 2D-modelling of the thermal evolution of Carboniferous and Devonian sedimentary rocks of the eastern Ruhr basin and northern Rhenish Massif, Germany. *Z. Dtsch. Geol. Ges.* **1995**, *146*, 321–339. [CrossRef]
39. Shalaby, M.R.; Hakimi, M.H.; Abdullah, W.H. Geochemical characteristics and hydrocarbon generation modeling of the Jurassic source rocks in the Shoushan Basin, north Western Desert, Egypt. *Mar. Pet. Geol.* **2011**, *28*, 1611–1624. [CrossRef]

40. Cohen, K.M.; Finney, S.C.; Gibbard, P.L.; Fan, J.X. The ICS international chronostratigraphic chart. *Episodes* **2013**, *36*, 199–204. [CrossRef] [PubMed]
41. Peng, Z.M.; Peng, S.M.; Wu, Z.P.; Li, W.; Kong, X. Evolution of the Jurassic–Cretaceous basins in the eastern part of North China and its response to the tectonic movement. *J. Southwest Pet. Univ.* **2009**, *24*, 7–12. (In Chinese)
42. Peng, Z.M.; Peng, S.M.; Wu, Z.P.; Li, W.; Kong, X. Rototype basin and the evolution in jurassic and cretaceous in eastern north china. *J. Southwest Pet. Univ.* **2009**, *31*, 37–42. (In Chinese)
43. Wang, M.J.; Zhang, X.H.; Zhang, Y.B. Restoration of Denuded Formation Thickness and Prototype Basin of Early to Middle Jurassic in Eastern Linqing Depression. *Spec. Oil Gas Reserv.* **2012**, *19*, 17–21. (In Chinese)
44. *DZ/T0216-2020*; Regulation of Coalbed Methane Reserves Estimation. China Standard Press: Beijing, China, 2020.
45. Liang, J.S.; Wang, C.W.; Liu, Y.H.; Gao, Y.J.; Du, J.F.; Feng, R.Y.; Zhu, X.S.; Yu, J. Study on the tight gas accumulation conditions and exploration potential in the Qinshui Basin. *Nat. Gas. Geosci.* **2015**, *25*, 1509–1519. (In Chinese)
46. Zhang, X.D.; Zhu, C.H.; Lin, J.F.; Xu, Y.K.; Wang, K. Geological reservoir properties of coal measures gas in Maqiao survey area of eastern Henan province. *J. Henan Polytech. Univ. (Nat. Sci.)* **2018**, *37*, 40–46. (In Chinese)